

## Dual Emission of 4-(1*H*-Pyrrol-1-yl)benzotrile Clusters with Acetonitrile in a Supersonic Jet and Its Absence in Phenylpyrrole Clusters

Leonid Belau and Yehuda Haas\*

Department of Physical Chemistry and the Farkas Center for Light Induced Processes, The Hebrew University of Jerusalem, Jerusalem, Israel

Wolfgang Rettig

Humboldt University of Berlin, Brook-Taylor-Str. 2, D-12489 Berlin, Germany

Received: November 20, 2003; In Final Form: January 20, 2004

The fluorescence of clusters of 4-(1*H*-pyrrol-1-yl)benzotrile (PBN) and of phenylpyrrole with acetonitrile (AN) was studied in a supersonic jet. Two separate bands are found in the case of PBN/AN clusters, one centered at 305 nm, the other at 450 nm. The blue- and red-shifted bands are assigned to locally excited (LE) and charge transfer (CT) states, respectively, in analogy with solution spectra of PBN in acetonitrile. The CT emission is observed only when mass spectra obtained upon resonance-enhanced multiphoton ionization (REMPI) of the clusters contain cluster ions in which at least four acetonitrile molecules are attached to a PBN molecule. In contrast, only a single emission band centered at 300 nm (assigned to a LE state) is observed from clusters of 1-phenyl-1*H*-pyrrole (PP) with acetonitrile prepared under similar conditions, regardless of cluster size. REMPI-induced mass spectra measured in coincidence with the fluorescence reveal a similar distribution of cluster sizes for the two phenylpyrrol derivatives. A possible rationalization for the different emission profiles is discussed in terms of excited-state dynamics.

### I. Introduction

PP and PBN belong to a class of molecules known to exhibit dual fluorescence in liquid solvents. This phenomenon, which was first observed for DMABN (dimethylamniobenzotrile),<sup>1,2</sup> is assigned to the existence of two minima on the surface of the first singlet excited-state  $S_1$ .

The nature of the two fluorescence bands has been extensively discussed but still appears to be controversial. Several models were advanced [see ref 2 for discussion]. Lippert's original hypothesis<sup>1</sup> was that there are two low-lying electronically excited states in the system, usually termed the A and B states. In the gas phase and in nonpolar solvents, the B state is lower in energy and is the only emitting state. The B state is the lowest excited state in the Franck–Condon region, and therefore initial vertical excitation always populates it preferentially. Emission from this state bears an approximate mirror image relationship to the absorption spectrum; this band is commonly termed the “normal” emission band. The “anomalous” fluorescence, which appears only in polar solvents and is strongly red shifted with respect to the absorption spectrum, is assigned to a charge transfer (CT) state. The B state is an essentially locally excited (LE) state of the benzene ring, related to the  $1^1B_{2u}$  state of benzene. The A state is a charge transfer (CT) state, related to the second excited state of benzene,  $1^1B_{1u}$ .

The basic assumptions of the model are still considered valid, but the exact nature of the A state, which is a charge transfer state, is still controversial. The leading current models are the TICT (twisted intramolecular charge transfer) model of Grabowski,<sup>3</sup> which assumes a twisted structure for the A state, and the PICT model of Zachariasse,<sup>4</sup> assuming a planar structure for the A state.

Many theoretical papers tried to simulate the excited states involved starting with the gas-phase molecule, for which high-

level calculations are available.<sup>5–8</sup> Since the A state emission is not observed in the bare molecule, a proper description must explicitly take into account the interaction with the solvent, as has been done for some systems with use of various models.<sup>7,9–11</sup> Most of the published work deals with DMABN, which was extensively studied experimentally and theoretically,<sup>2</sup> making it a standard “parent” molecule that is used to discuss properties of other benzene derivatives that display dual fluorescence.

Small clusters, easily prepared in a supersonic jet, are in principle simpler to analyze than a macroscopic system. In recent years, much progress has been made toward first principles understanding of the structure and binding in these clusters.<sup>12</sup> Powerful theoretical methods, including ab initio calculations, are being applied to characterize their structures and energy level diagrams. In the hope that the experimental study of such clusters might elucidate the nature of the dual emission, several groups tried to observe the “anomalous” emission in supersonic jets.

Reported results on the fluorescence of DMABN co-expanded in a supersonic jet with polar molecules convey a conflicting story. Howell et al.<sup>13</sup> observed dual fluorescence from such systems, but assigned the red-shifted band to a dimer of DMABN. No emission from the monomer complexed with AN or other polar molecules was observed. Krauss et al.<sup>14</sup> reported dual emission from  $DMABN \cdot (AN)_n$  clusters for  $n \geq 5$ . This result was based on the simultaneous recording of fluorescence and resonance enhanced multiphoton ionization (REMPI) mass spectra. In addition to the LE band around 345 nm, they observed an emission band around 425 nm, which was assigned to CT emission based on its similarity to the solution phase spectra. In contrast, Saigusa et al.,<sup>15</sup> using very similar apparatus, failed to observe the red-shifted emission from either DMABN/water or DMABN/acetonitrile clusters, even though the REMPI

mass spectra indicated the existence of large clusters. Saigusa et al. proposed that the red-shifted emission observed in ref 14 was due to clusters of DMABN dimers, which were also present in the jet.

The pyrrolo group is a better electron donor than the dimethylamino one; consequently dual emission is observed from PP in polar solvents such as AN<sup>16</sup> but not from *N,N*-dimethylaniline. Nonetheless, the weaker electron-attracting power of the phenyl ring compared to the cyanophenyl one is revealed by the fact that while for DMABN and PBN<sup>17,18</sup> the CT emission band is the only observed one in solvents more polar than alkanes at room temperature, in the case of PP the CT emission appears only as a shoulder on the red side of the LE emission in polar solvents such as AN. We have recently observed dual emission from PP in an argon matrix doped by acetonitrile.<sup>19,39</sup> The emission spectrum depended strongly on excitation conditions, but the two bands were found to be well separated under proper conditions, with the LE emission peaking at 300 nm and the CT one at 345 nm. In contrast, PBN was found to exhibit only a single rather broad emission band under similar conditions.<sup>19</sup> These results indicate that in cold environments the system may be kinetically (rather than thermodynamically) controlled. It therefore appeared instructive to investigate the properties of clusters of the pyrrole derivatives PP and PBN with polar molecules in a supersonic jet expansion, where the relative motion of the molecules is much less restricted.

This paper reports the first study of PP and PBN clusters in a supersonic jet. Our data show that PBN·(AN)<sub>*n*</sub> clusters do exhibit dual emission (for *n* ≥ 4), as well as clusters of PBN dimers. However, no dual emission was observed from PP clusters with AN of any size. The possible reasons for these findings and their bearing on the origin of the dual fluorescence are discussed.

## II. Experimental Section

The experimental setup is a modification of the setup described in ref 22. The vacuum chamber consisted of a 6 in. stainless steel (SS) cross joined to a 6 in. SS Tee. The SS cross was pumped by a 6 in. diffusion pump (Varian VHS4) and the SS Tee by a 350 L/s turbomolecular pump (Leybold, Turbovac 361C). A supersonic jet was formed by expanding a gas mixture through a pulsed valve (General Valve Co., G9, 0.7 mm nozzle diameter) into the cross. The jet was skimmed by a skimmer placed between the cross and the Tee (Beam Dynamics, 2 mm diameter) forming a molecular beam. The background pressure in the system was 10<sup>-8</sup> Torr, with the valve closed. When the valve was operated at 10 Hz, the pressure in the cross was around 10<sup>-6</sup> Torr, and that in the Tee was 10<sup>-8</sup> Torr. A Wiley–McLaren time-of-flight mass spectrometer (TOFMS) was connected to the TEE.<sup>20</sup> The flight tube (1.3 m long, 10 cm diameter) was pumped by an additional turbomolecular pump (Alcatel, CIT 5150, 120 L/s).

Ions were created in the source of the TOFMS by multiphoton absorption of a frequency doubled dye laser (Lambda Physic DL3002 Spectral resolution 0.4 cm<sup>-1</sup>) pumped by an excimer laser (Lambda Physic EMG101MSC, 10 ns pulse width). The ions are deflected perpendicular to the molecular and laser beams, passed through an electrostatic deflector to compensate for the translational motion of the parent neutrals, and monitored by a Daly-type detector. The laser beam passed through the Tee and was then directed into the SS cross, intersecting the molecular beam 10 mm down stream from the nozzle. The fluorescence excited this way was dispersed by a 1/3 m monochromator (Jobin Yvon, SPEX 340E) and detected by a

photomultiplier tube (PM) (Hamamatsu R928). This arrangement ensured that the mass spectrum and the fluorescence were excited by the same laser pulse. REMPI and fluorescence signals were digitized by oscilloscope (Tektronix, TDS 620B 500 MHz). The whole experiment was controlled by a personal computer with use of LabView software (National Instruments, 6.i). The timing sequence and control was by a digital delay generator (SRS model DG535). Decay times were measured by feeding the PM current into a 50 Ω terminator and fitting the resulting decay curve to an exponential function. Extensive signal averaging was employed when necessary until an acceptable S/N ratio was obtained. The overall time resolution of the equipment is estimated at 7 ns.

PP (Aldrich, 99%) was used as received. PBN was prepared as previously described.<sup>21</sup> Spectrophotometric grade acetonitrile (Aldrich, 99.5+%) and methanol (J.T.Baker, 99%) were used as received. PP or PBN crystals were placed in a small oven next to the nozzle and their vapor pressure was controlled by adjusting the oven's temperature. The vapor of the organic solvent was mixed with helium in the desired ratio in a constant pressure reservoir,<sup>22</sup> and the mixture was passed over the heated crystals before being expanded in the nozzle.

## III. Results

**III.a. PBN Clusters.** The emission spectrum and REMPI mass spectrum recorded when PBN vapor is expanded in a helium supersonic jet and excited at the origin band (290.49 nm) are shown in Figure 1. Addition of acetonitrile (AN) to the gas mixture leads to different spectra, as illustrated in Figure 2. Under these conditions, excitation at the origin band leads also to vibrationally structured emission spectrum around 305 nm (the “blue” band) but in addition a broad and structureless band is observed around 460 nm (the “red” band). A detailed comparison of the blue band with the one observed in Figure 1 is not feasible, as the S/N ratio did not allow the use of the same resolution. It should be recalled that under the conditions of the experiments shown in Figure 2, a considerable fraction of the PBN molecules are not bound to AN, so that the blue band contains possible contributions from bare and bound PBN molecules. The REMPI spectrum of Figure 2 contains several new mass peaks, corresponding to [PBN·(AN)<sub>*n*</sub>]<sup>+</sup> cluster ions with *n* = 1–16.<sup>23</sup> Setting the excitation wavelength a little to the red of the 0,0 band of bare PBN (291 nm, where no monomer absorption takes place<sup>24</sup>), the 460 nm emission band persists, but the 305 nm one is barely perceptible. The spectra obtained upon excitation at 291 nm must be due to PBN·(AN)<sub>*n*</sub> clusters as no signal is obtained when either PBN or AN is expanded in the helium jet under these conditions. The excitation spectra of the red band and of the [PBN·(AN)<sub>*n*</sub>]<sup>+</sup> mass peaks (*n* = 0–5) are shown in Figure 3. They are remarkably similar, almost completely devoid of vibrational structure. Close inspection indicates that the action spectrum of the [PBN·(AN)<sub>5</sub>]<sup>+</sup> mass peak is somewhat different from the others. It is clear from the figure (panel B) that under the conditions of the experiment, both the 305-nm band (apart from bare PBN lines) and the 460-nm band arise from clusters. Moreover, the excitation spectra giving rise to these two bands are very similar.

The fluorescence and mass spectra were found to strongly depend on the expansion conditions as shown in Figure 4. Varying the AN pressure, the cluster-size distribution (as measured by the mass spectrum) can be changed progressively; the bottom panel shows that under conditions such that only [PBN·(AN)<sub>*n*</sub>]<sup>+</sup> cluster ions where *n* ≤ 3 appear in the mass spectrum, the 305-nm fluorescence emission band is the only

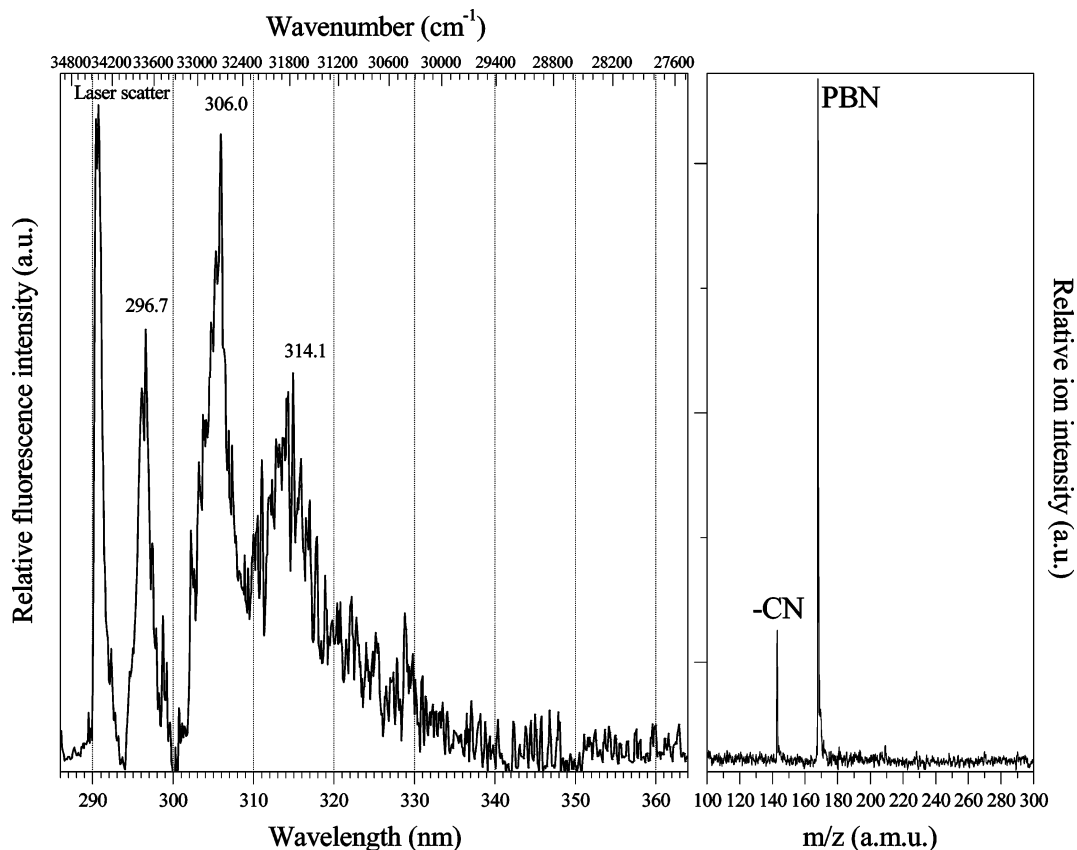


**Figure 1.** The fluorescence spectrum (left, spectral resolution  $160\text{ cm}^{-1}$ ) and the simultaneously recorded time-of-flight mass spectra (TOFMS) of PBN in a supersonic jet. Excitation is at the 0,0 band ( $290.49\text{ nm}$ ), the oven temperature was  $393\text{ K}$ , and the helium pressure was  $7\text{ atm}$ . The  $168\text{-amu}$  band is assigned to the parent PBN and the  $142\text{-amu}$  peak to a fragment ion after the loss of a CN radical (smaller fragments, not shown in the figure, are also observed). The first vibronic band contains a contribution from the scattered laser light. The decay time measured for the fluorescence was  $16 \pm 1\text{ ns}$ .

one observed. The next panel shows that when  $[\text{PBN}\cdot(\text{AN})_4]^+$  mass peaks are additionally present in the REMPI spectrum, the  $460\text{-nm}$  band becomes weakly observable. Its intensity relative to that of the  $305\text{-nm}$  band increases upon increasing AN pressure, until it almost completely dominates the spectrum at the highest AN pressure used (second panel from top). The resulting emission spectrum is very similar to the spectrum of PBN dissolved in acetonitrile (top panel). The corresponding mass spectra are independent of the excitation wavelength, as long as only clusters (not the bare molecule) are excited. Mass peaks corresponding to  $[(\text{PBN})_2\cdot(\text{AN})_n]^+$  are also observed under these conditions.

The fluorescence signals of both the blue and red bands appeared to decay exponentially under all experimental conditions. This result is surprising, as emission in both cases is expected to be due to a distribution of clusters of various sizes and structures. Attempts to discern a nonexponential decay by improving the signal-to-noise ratio using extensive averaging did not lead to a better fit. Therefore, the data are analyzed by using a single-exponential fit, which is understood to represent some average decay time. Figure 5 shows a typical decay curve and the measured decay times as a function of the emission wavelength recorded for two different expansion conditions. Several trends are noted: (i) The decay time is much shorter for the  $305\text{-nm}$  band than for the  $460\text{-nm}$  one. (ii) A gradual increase of the lifetime is observed for the  $460\text{-nm}$  band for longer emission wavelengths, which appears to level off around  $26\text{ ns}$  at the longest wavelengths. (iii) A small but persistent difference between the high and low AN pressure data is observed: at lower AN pressure the lifetime in the CT band is

$10\text{--}15\%$  longer. Furthermore, a gradual red shift as the observation window is set to longer delay times is observed.

Some experiments were run with methanol (MeOH) as the added gas. The results are qualitatively similar, but the data appear to indicate possible chemical reaction between PBN and methanol, and will not be further discussed in this paper. We only mention that as in the case of AN clusters, two separate bands were observed, one assigned to a LE transition, the other to a CT one. However, at high methanol pressures the spectrum did not converge to the solution-phase spectrum.

**III.b. PP Clusters.** The emission spectra and REMPI mass spectra recorded when PP was co-expanded with AN in a helium supersonic jet are shown in Figure 6 for several excitation wavelengths. The fluorescence spectrum in all cases is centered at about  $300\text{ nm}$ . Near the origin of the  $S_0\text{--}S_1$  transition of the parent molecule, the spectrum displays clearly resolved vibronic structure, which disappears upon excitation at higher energies. No indication for a second emission band in the  $350\text{--}400\text{-nm}$  range (as expected from solution<sup>16</sup> and matrix<sup>19</sup> spectra) was found, despite extensive searching. In contrast with the case of PBN, emission spectra due to large clusters (whose presence in the jet is confirmed by the mass spectrum) do not correlate well with the liquid solution spectrum. In an attempt to check whether a barrier for CT formation must be exceeded, emission and mass spectra were recorded at different excitation wavelengths. However, no sign of a red-shifted band (or even shoulder) could be traced.

The ion cluster-size distribution as a function of increased AN pressure in the preexpanded mixture was comparable to that observed for PBN under similar expansion conditions: at

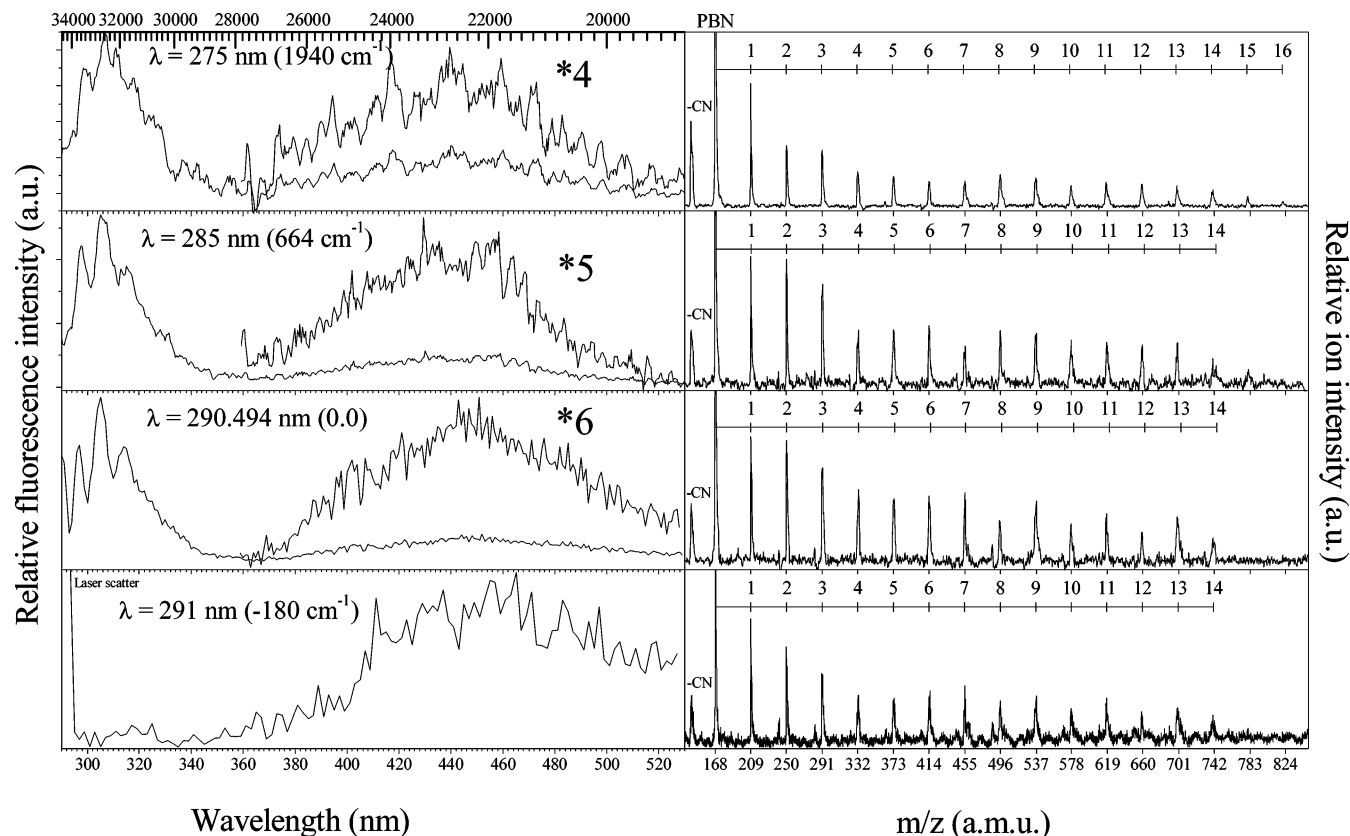


**Figure 2.** Left panels: Emission spectra obtained from a mixture of PBN and AN co-expanded in a helium jet upon excitation near the 0,0 band of bare PBN (nozzle temperature 372 K; AN pressure 12 Torr; helium pressure 5 atm). Spectral resolution was  $320\text{ cm}^{-1}$ . Right panels: Time-of-flight mass spectra (TOFMS) recorded simultaneously with the fluorescence spectra (identical expansion and laser excitation conditions). The numbers over the ion peaks indicate the number of AN molecules attached to PBN. The excitation wavelengths (nm) are indicated in the left-hand part, along with the excess energy ( $\text{cm}^{-1}$ ) relative to the 0,0 band of bare PBN (290.49 nm). The bottom panels show the results of excitation slightly off resonance (at 291 nm). At this wavelength PBN monomers have no absorption and no LE fluorescence is observed.

high pressures large clusters (at least up to 15 AN molecules attached to 1 PP molecule) were observed.

The fluorescence excitation spectrum near the origin of the 0,0 band of bare PP is shown in Figure 7, along with the action spectra of some  $[\text{PP}\cdot(\text{AN})_n]^+$  ions. The parent ion mass peak action spectrum at  $m/z$  143 is seen to have a distinct vibrational structure, with very little underlying continuum. In contrast, the fluorescence excitation spectrum, while showing exactly the same vibronic structure, is superimposed on a slowly rising continuous background. This indicates that fluorescence is observed from both bare molecules (narrow features) and clusters (quasicontinuous background), but the molecular parent ion peak at  $m/z$  143 amu is due almost exclusively to the excitation of the bare neutral. For the larger ion peaks ( $n \geq 1$ ), the signal-to-noise ratio is not good enough to discern structure, but the overall shape of the spectrum is seen to be similar to the continuum background of the fluorescence, with some blue shift.

A few experiments were run with methanol (MeOH) as the ligand. The formation of  $\text{PP}\cdot(\text{MeOH})_n$  clusters proved to be less efficient than that for  $\text{PP}\cdot(\text{AN})_n$  clusters. Only a few cluster ions are observed, with the most intense peaks for the  $n = 4$  and 5 cluster ions. The emission spectrum shows a small red shift as the excitation energy is increased. In contrast with the case of PBN/MeOH clusters, no separate new emission band is observed above 350 nm.

#### IV. Discussion

**IV.a. Summary of the Experimental Results.** The main result of this work is the fact that clusters of  $\text{PBN}\cdot(\text{AN})_n$  ( $n \geq$

4) exhibit dual fluorescence, while  $\text{PP}\cdot(\text{AN})_n$  clusters do not for any  $n$ . Modeling of the system has to consider the following experimental data.

*For PBN:* (1) The excitation spectra of the blue and red emission bands are rather similar. Near the origin of the 0,0 transition of the bare molecule vibrational structure is discerned in the blue band, but not in the red one, nor in the cluster-ions action spectrum. On the other hand, the red-band emission is preferentially observed upon excitation off-resonance of the bare molecule transitions. Excitation to the red of the 0,0 band of the bare molecule leads to red-band emission only. (2) The rise times of both bands are within the time resolution of the experiments ( $\sim 7$  ns). (3) The decay times are nearly exponential for both bands. They are  $12 \pm 2$  ns for the blue band and longer for the red one. In the case of the latter, the decay time increases with increasing wavelength, reaching a value of  $26 \pm 2$  ns at 480 nm. (4) The red band's intensity relative to that of the blue one increases as the acetonitrile content in the expanding mixture is increased. An increase in the abundance of large cluster ions in the mass spectrum is observed concurrently.

*For PP:* (5) In the case of PP, with AN pressures similar to those employed with PBN, ion clusters of similar sizes were observed, but no red-shifted band was detected. At fixed AN pressure, excitation at shorter wavelengths leads to an increase of the larger cluster ions formed, but no red-shifted emission is observed. It is recalled that in liquid solutions and AN-doped argon matrices, red-band emission is observed.

**IV.b. The Identity of the Emitting Species.** The large number of cluster ions observed by the REMPI technique for

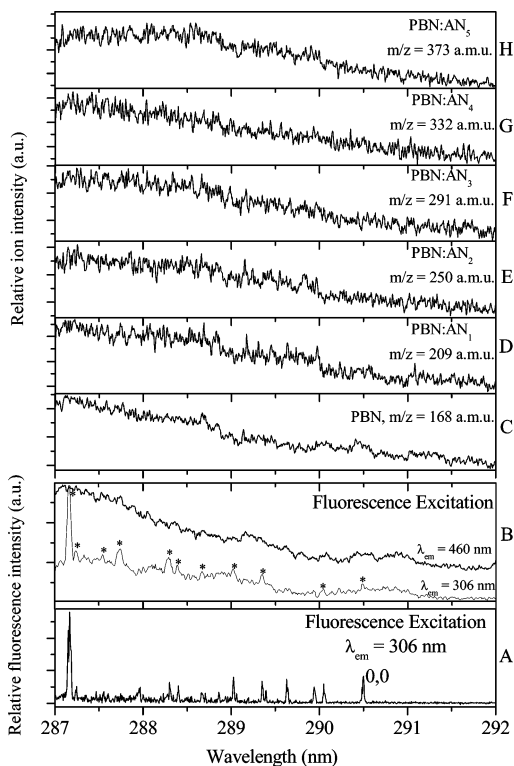


**Figure 3.** Fluorescence excitation spectra (panel A: PBN only,  $\lambda_{em} = 306$  nm; panel B: PBN co-expanded with AN,  $\lambda_{em} = 460$  nm, spectral resolution set to  $800\text{ cm}^{-1}$ ). Panels C–H: Mass resolved excitation spectra of selected ions obtained in a supersonic expansion of PBN and AN in helium jets. Oven temperature 392 K; AN pressure 12 Torr; helium pressure 5.5 atm. Cluster composition is expressed as  $(\text{PBN}\cdot\text{AN}_n)$  where  $n$  is the number of AN molecules in the cluster.

both PBN and PP clearly implies a broad distribution of neutral clusters in the supersonic jet. These clusters, which vary in size and structure, are responsible for the observed red emission band in the case of PBN. The blue band arises partly from bare molecules and partly from clusters. A pertinent question is whether the blue and red bands are due to the same ground-state precursors. Evidently, small clusters do not emit at the red band (Figure 4), but at present the data do not allow the dissection of the observed emission to spectra due to individual clusters.

A schematic energy level diagram of the system is presented in Figure 8. In the bare molecule, the CT state lies at a higher energy than the LE state. Initial excitation is preferred (mainly by Franck–Condon considerations) to the LE state (a molecule in this state is denoted by  $\text{P}^*$ ). At low excitation energies nonradiative transitions are unlikely and only “normal” (LE-type) fluorescence is observed upon excitation of  $\text{P}^*$ . When a high-power laser is used for excitation, resonance-enhanced absorption of a second photon during the lifetime of the excited state can lead to ionization, which is observed for both PP and PBN. The biggest ion observed when only PP or PBN is expanded in helium is the parent ion. Smaller ions due to fragmentation of the parent are also observed; for instance in the case of PBN, a peak at 142 amu is also observed, which is assigned to the loss of the CN group from the neutral molecule.

When the molecule is van der Waals bound to one or more ligands, the energies of all electronic states are lowered. In general, excited states are stabilized to a larger extent than the ground state, causing a red shift in the absorption spectrum. The LE state is still Franck–Condon preferred, but direct excitation of the CT state (denoted by  $\text{P}^{\text{CT}L_k}$ ) should also be considered, as the bottom panel of Figure 2 shows that at

frequencies smaller than the 0,0 transition of the bare molecule red-shifted emission can be excited without any sign of LE-type fluorescence. The CT state is stabilized to a bigger extent than the LE state by polar molecules attached to the PBN, and with a large enough number of polar ligands attached, the energy ordering appears to be reversed: the CT state (at its equilibrium geometry) is lower than the LE state. This makes possible a nonradiative transition converting an initially excited LE cluster to a CT one. However, it is likely that a barrier has to be overcome in the process (energy barriers are not shown in Figure 8). Therefore, an excess energy may have to be pumped into the LE cluster: a vibrationally excited  $\text{P}^*L_n(v)$  cluster may have the energy required to overcome the barrier and to form a  $\text{P}^{\text{CT}L_k}$  cluster ( $k \leq n$ ). This process could be accompanied by “evaporation” of one or more ligand molecules. Another possible process is the dissociation of  $\text{P}^*L_n(v)$  to smaller clusters  $\text{P}^*L_m(v')$ . Still another possibility is the absorption of a second photon leading to ionization. Ionization of the  $\text{P}^{\text{CT}L_k}$  clusters is also possible (see the bottom panel of Figure 2). Processes following initial excitation of a vibrationally excited LE state are summarized in the following simplified kinetic scheme (possible transitions to the triplet state are ignored). In addition, red-band emission due to direct excitation of the CT band and emission from noncomplexed  $\text{P}^*$  molecules are observed. We have neglected the back reaction converting  $\text{P}^{\text{CT}}$  clusters to  $\text{P}^*$  ones, assuming that the CT state lies at lower energy due to evaporative cooling.<sup>25</sup>

**IV.c. Size Dependence of LE and CT Emission.** The detailed energy requirements for the different processes could not be established for this system (in contrast with others<sup>22,26</sup>), as the excitation spectra are devoid of vibrational structure. The congested character of the spectrum (recall that the systems are jet-cooled) is most probably due to overlap between slightly different absorption spectra due to several clusters differing in size and structure. Thus it is assumed that the solvent shift of LE-type clusters as a function of the number of attached ligands (or geometry) is small (otherwise, discrete absorption peaks would have been observed). A qualitative estimate of the energy stabilization may be made, however, by considering typical values of cluster bond dissociation energies (BDEs) that are known for systems of similar size. Table 1 summarizes some results on BDEs of some clusters in their ground state and cluster ions.

It is evident that the binding energies of van der Waals complexes in the ground state are much smaller than the BDE of the same pairs with one electron removed (ion clusters). This is due to the added electrostatic interaction that is stronger than the dispersion forces holding together the neutral clusters. In contrast, bond dissociation energies of the LE states of clusters are usually quite close to those of the ground-state ones.<sup>26,29–32</sup> It is also evident that the ionization potential of clusters is usually lower than that of the bare molecule by 0.2 to 0.7 eV (5 to 16 kcal/mol). Therefore, multiphoton excitation of clusters near the 0,0 band of the bare monomer can lead to ionization of the cluster, depositing a large energy excess in the cluster ion compared to van der Waals binding energies. This may lead to the dissociation of the cluster ion. In particular, under these conditions it is possible to observe the bare molecule ion signal even at excitation frequencies that are not resonant with any bare molecule transition. At 291 nm the cold bare PBN molecule does not absorb, so that the  $\text{PBN}^+$  ion observed must be due to a fragment of a cluster ion (cf. Figure 2).

The binding energies of a cluster in the CT state are expected to be larger than those of the clusters of LE molecules as the

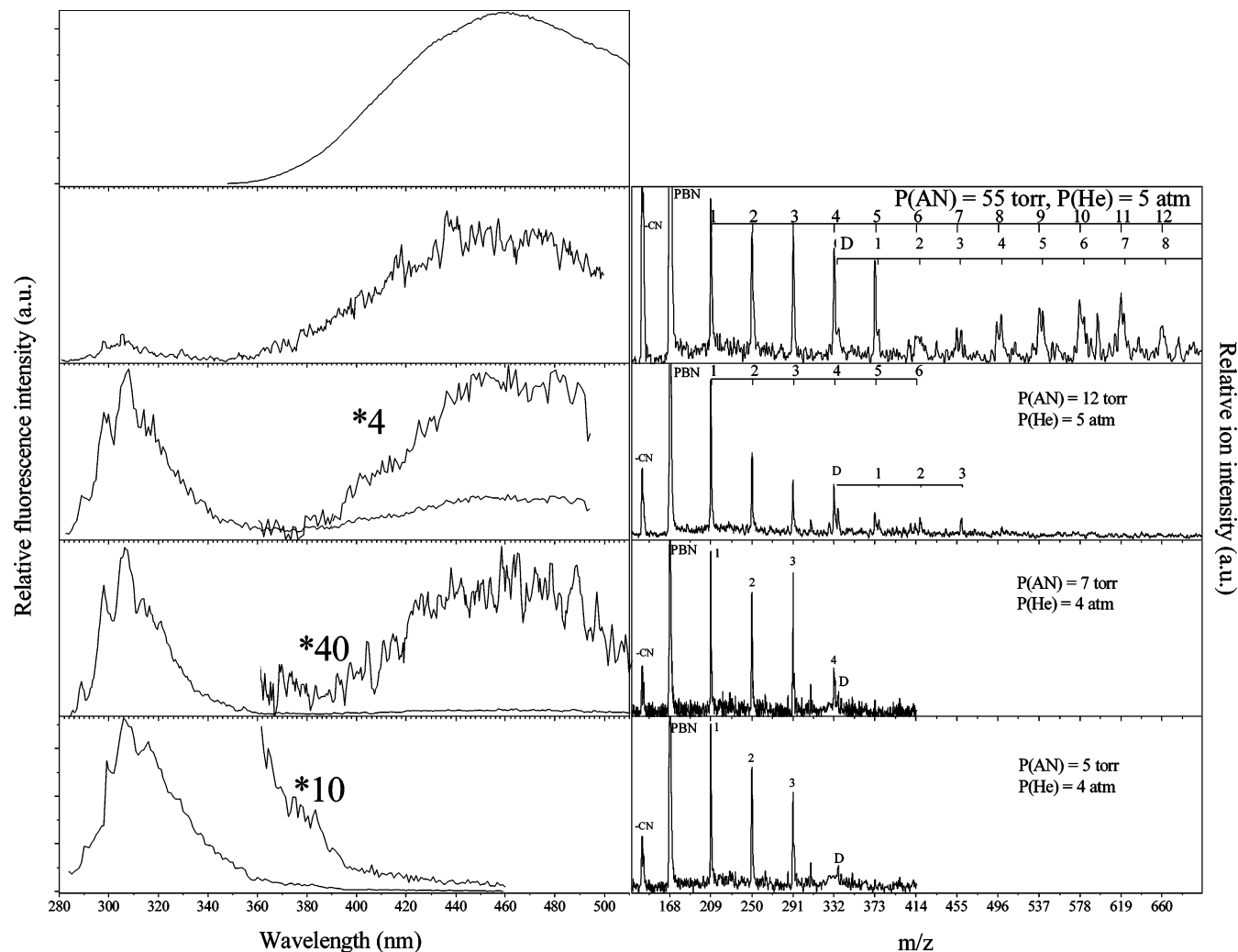


**Figure 4.** The effect of AN pressure and of expansion conditions on the fluorescence and cluster size distribution of co-expanded PBN and AN in helium jets. Oven temperature 399 K; excitation wavelength 285 nm; AN and helium pressures were adjusted to get the desired cluster size distribution. PBN dimers are indicated by the symbol D. The top panel shows the emission spectrum of PBN dissolved in acetonitrile at room temperature.

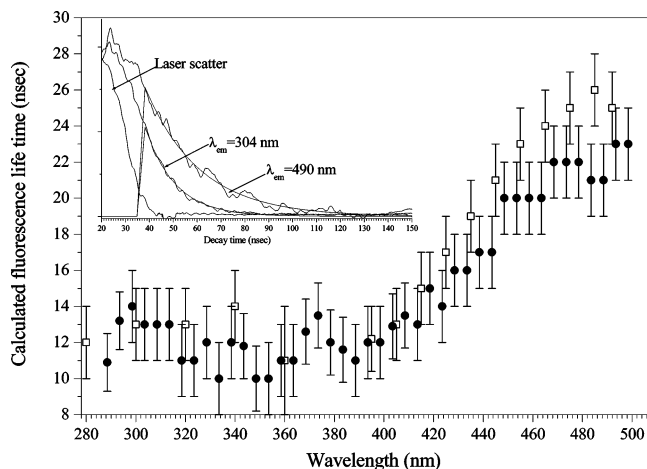


**Figure 5.** The measured decay times (assumed single exponential) as a function of emission wavelength for PBN·AN clusters: filled circles, AN pressure 55 Torr; open squares, AN pressure 7 Torr. The inset shows two examples of the actual decays, plotted with the fitted curves. The main source of error is due to the noise level of the baseline. The error bars indicate the two limiting cases taken for the baseline.

charges are separated in the pyrrolbenzene derivative and the dipole moment of the ligand is large. Charge-transfer resonance interaction is also known to stabilize charged dimers.

The structure of jet-cooled van der Waals adducts has been extensively discussed.<sup>12</sup> It is well-known that in a large adduct,<sup>32</sup> ligands can bind to benzene and its derivatives either in several attachment points or as a cluster at one point. Each cluster is characterized by a specific absorption spectrum, which is only slightly shifted in energy with respect to the others.

**IV.d. Application to PP and PBN.** In the bare molecule, the LE excited state lies at a lower energy than the charge transfer state. CASPT2 calculations predict an energy gap of 12.65 and 4.6 kcal/mol for the quinoid CT state (Q-form) of PP and PBN, respectively.<sup>8</sup> For the antiquinoid CT state (anti-Q form) the calculated gaps in the isolated molecules are much larger: 28 and 30 kcal/mol for PP and PBN, respectively. At this point it is difficult to estimate the error in the CASPT2 calculations; for the moment we shall use the lower energy Q-form for the analysis. The calculated dipole moments of the Q-forms of PP and PBN are 0.7 and 11.0, respectively.

The following data are available from room temperature solution spectra:<sup>17,18</sup> The LE emission is centered at 300 and 330 nm for PP and PBN in alkane solvents, respectively. The CT band, observed in liquid AN, is centered on 360 and 450 nm for these two molecules. The red shift is thus about 16 and 30 kcal/mol for PP and PBN, respectively. As the temperature is lowered, the relative intensity of the CT band is increased. By reference to Figure 9, the red shift of the CT band arises

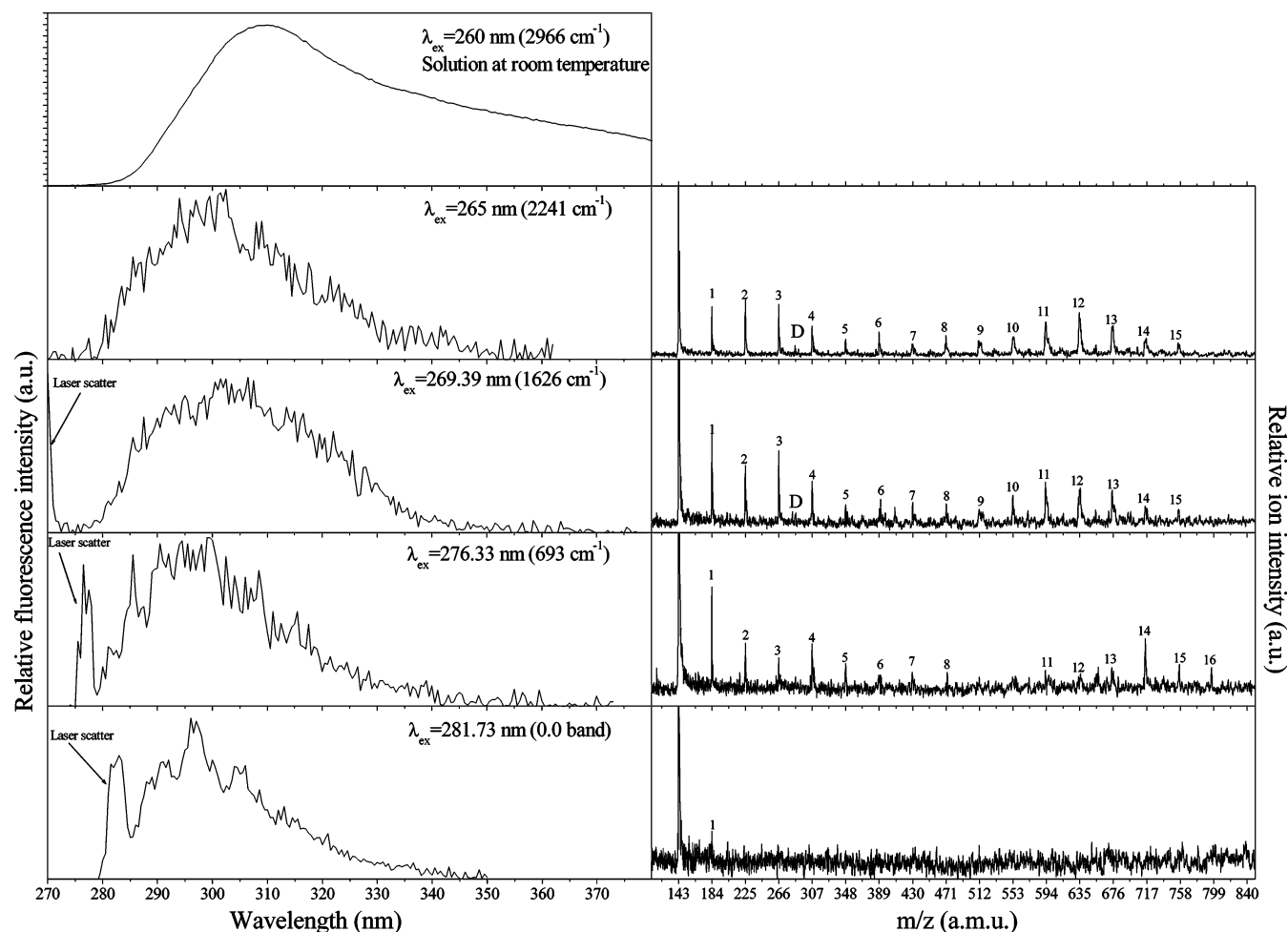


**Figure 6.** The effect of excitation wavelength on the fluorescence and REMPI induced cluster size distribution of co-expanded PP and AN in helium jets. The deflection correction was not applied in the REMPI spectra shown; the mass spectrum of the clusters is actually independent of excitation wavelength. Oven temperature 342 K; AN pressure 70 Torr; helium pressure 7 atm. The top panel shows the emission spectrum of PP dissolved in acetonitrile at room temperature (the spectrum consists of two overlapping bands, assigned to LE and CT transitions). The numbers in parentheses indicate excess energy over the 0,0 band of bare PP.

from two effects: the excited-state stabilizing contribution  $\Delta E^*$  and the ground-state destabilizing contribution  $\Delta E^\circ$ . Assuming an equal contribution from these two effects,<sup>33</sup>  $\Delta E^*$  turns out to be about 15 kcal/mol for PBN and 8 kcal/mol for PP. This estimate is in good agreement with the expected stabilization of a dipole in a polar solvent such as acetonitrile, using Onsager's reaction field theory (0.6 eV for  $\mu=16$  D,  $\epsilon$ (dielectric constant) = 39).<sup>34</sup>

A prerequisite for the conversion of a LE cluster  $P^*L_n$  to a CT cluster  $P^{CT}L_n$  under collision-free conditions is that the latter should be of lower energy. Assuming roughly that each attached AN molecule in the first solvation layer contributes equally to the stabilization and that PBN can be solvated by 4–6 nearest neighbors, an extra stabilization of about 3–4 kcal/mol per AN molecule is expected to lead to a 20 kcal/mol total stabilization of the CT cluster compared to the LE one. In the case of PP the stabilization by a polar molecule is much smaller and consequently the driving force for intracuster  $P^*L_n \rightarrow P^{CT}L_n$  transformation is smaller or the reaction may be even endoergic, and the reaction rate constant is consequently smaller, too. In this case it may become smaller than the rate constant for ligand dissociation, and only LE emission is expected, as observed experimentally.

Some support for the kinetic scheme of eqs 1–5 comes from the measured decay times presented in Figure 5. The decay times of both the LE and CT states could be fitted with a single

exponential decay, although emission is most probably due to an ensemble of different clusters. The locally excited clusters, regardless of size, appear to decay with a shorter lifetime than the bare molecule ( $12 \pm 2$  ns, compared to  $17 \pm 1$  ns for the bare molecule<sup>24</sup>). The change could be due to a decrease in the natural lifetime, but can also be ascribed to added decay channels such as decomposition and enhanced internal conversion or intersystem crossing. A longer decay time is observed for clusters emitting in the red band. The decay time is seen from Figure 5 to increase with the emission wavelength, leveling off at around  $26 \pm 2$  ns for smaller clusters and  $22 \pm 2$  ns for the larger ones. The emissive transition is Franck–Condon forbidden in this case and should have a longer natural lifetime than that of the LE state. Within the red band, measurements in the longer wavelength region are more reliable for representing the true decay times of CT clusters, as at the shorter wavelengths some contribution from LE states cannot be ignored. In addition, the short wavelength decays may include a contribution from vibrationally excited CT clusters that have sufficient internal energy and can dissociate in competition with fluorescence. Such clusters are on average higher in energy than the vibrationally cool ones, and therefore have a larger contribution of shorter wavelength emission. Fragmentation can take place, but does not change the nature of the excited state: a smaller CT cluster results. Since the CT state is the lowest energy singlet excited state, complete loss of the solvent molecules necessarily leads

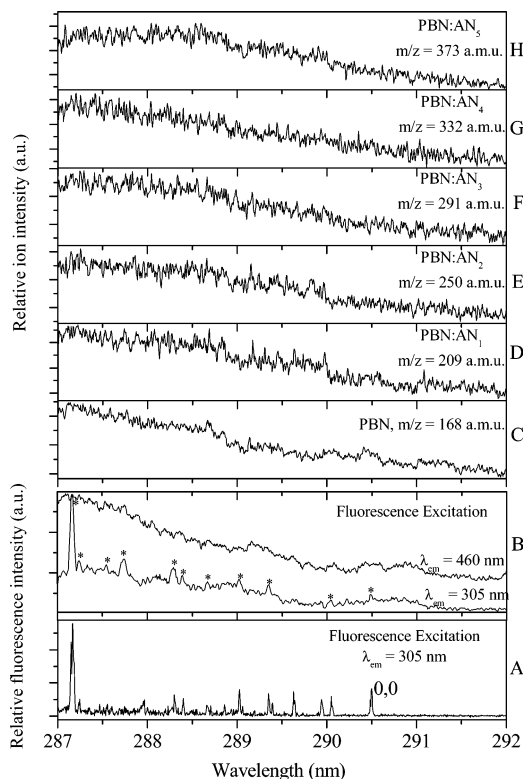


**Figure 7.** Fluorescence excitation spectra (bottom,  $\lambda_{em} = 300$  nm, spectral resolution  $800\text{ cm}^{-1}$ ) and mass resolved excitation spectra of selected ions obtained in a supersonic expansion of PP and AN in helium jets (top 6 spectra). Oven temperature 327 K, AN pressure 25 Torr, helium pressure 7 atm.

to the ground state (or the triplet state, which we did not observe). These processes appear to be minor under the conditions of the present experiments.

A point that requires further study is the *formation* rate of the CT state. The time resolution of our apparatus was not high enough to directly observe the rate of this process. If direct excitation is the major initiation process of this emission, a better time resolution will not make a difference. However, if  $k_{LE \rightarrow CT}$  is of the order of  $10^9\text{ s}^{-1}$  or greater, picosecond experiments might help to resolve this issue. Such large rate constants are observed in solution, but kinetic data are not available for temperatures of the order of 10 K prevailing in the supersonic jet. If indeed the second alternative holds, the barrier for the  $LE \rightarrow CT$  process must be very small for large clusters

Next, we consider the impact of the observed REMPI-induced mass spectra on the interpretation of the fluorescence spectra. The ionization energies of PP and PBN are 8.16 and 8.55 eV, respectively,<sup>35</sup> so that absorption of two photons in the range used in these experiments can lead to ionization. The cluster *ion* size distribution depends on the *neutral* size distribution prior to light absorption, but since at least two photons are required, the unknown absorption coefficient of the second photon also affects the observed ion distribution. Since the stabilization of molecular ions by polar molecules upon cluster formation is much larger than that of the neutral molecules, excitation near the origin of the bare molecule is expected to create cluster ions with a large excess energy, enough to exceed the bond dissociation energy of the cluster. The IP of the clusters is expected to be 10–20 kcal/mol lower than that of the bare molecule. The extra energy deposited in the cluster is large enough to cause the rupture of the van der Waals bond between the ion and one ligand, and can lead to the ejection of one or

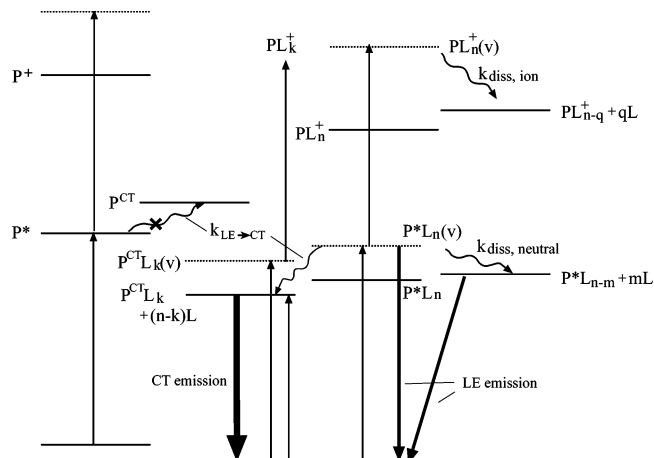


**Figure 8.** A schematic energy level diagram showing (left) the bare molecule. Right: A cluster of the molecule with acetonitrile (AN) ligands attached. The LE states are designated by a single asterisk ( $P^*$  denotes the bare molecule and  $P^*L_n$  a cluster with  $n$  ligands attached). The CT states are marked by the superscript CT ( $P^{CT}$  and  $P^{CT}L_k$ , respectively). Positive ions are denoted as  $P^+$  and  $PL_n^+$ .  $P^*L_n(v)$  denotes a vibrationally excited molecule in the LE state. The charge transfer state of the cluster can be formed either by direct absorption or by a radiationless transition from the LE state. The rate constant for isomerization of the  $P^*$  species to the  $P^{CT}$  one is  $k_{LE \rightarrow CT}$ . It is negligibly small (compared to  $k_f(LE)$ , see eq 4) for the bare molecule and big enough to compete with spontaneous emission for AN clusters with  $n \geq 4$ . Charge transfer emission (heavy downward arrow) is shifted to the red with respect to the LE emission (slimmer downward arrows). Direct absorption to the CT state is experimentally observed for PBN-(AN)<sub>n</sub> clusters but not for PP(AN)<sub>n</sub> ones. Absorption of a second photon from the excited states can lead to ionization, which may be followed by dissociation of the ion cluster. All clusters (neutral and ionic) may lose one or more ligands if vibrationally excited (rate constant  $k_{diss}$ ).

### SCHEME 1: A Kinetic Scheme of Cluster Dual Fluorescence

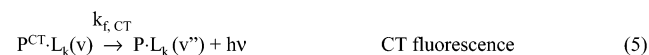


**TABLE 1: Energies (eV) of Some Clusters and Their Ions<sup>a</sup>**

components	IP (cluster)	IP (monomer)	DIP	BDE neutral	BDE cluster ion	ref
benzene/benzene	8.65	9.24 (B)	0.59	0.07	0.66	26
benzene/cyclohexane	9.12	9.24 (B)	0.12	0.08	0.20	26
benzene/toluene	8.34	8.83 (T)	0.49	0.15	0.53	26, 27
benzene/indole	7.42	7.77 (IN)	0.35	0.23	0.57	28
styrene/TMA	7.67	7.82 (TMA)	0.15	0.14	0.28	22

<sup>a</sup> IP: first ionization potential. DIP: difference between ionization potential of the monomer (initials in parentheses) and the cluster. BDE: bond dissociation energy.

more ligands, depending on the geometry of the cluster (Figure 10). Taking all these considerations into account, it is clear that the observed cluster ion distribution provides only a qualitative idea about the neutral size distribution. However, the largest observed ion in any given experiment is a lower limit for the



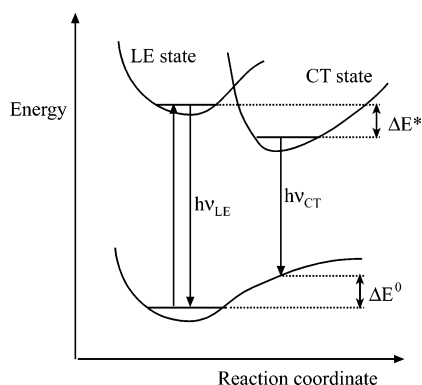


**Figure 9.** A schematic energy level diagram showing the relation between the emission frequencies and the stabilization of the cluster in the ground and in the excited states.  $\Delta E^\circ$  is the destabilization of the ground state at the optimized geometry of the solvated CT excited molecule and  $\Delta E^*$  is the stabilization of the CT state with respect to the LE excited states. The red shift of the CT emission is given approximately by the sum of these two contributions.

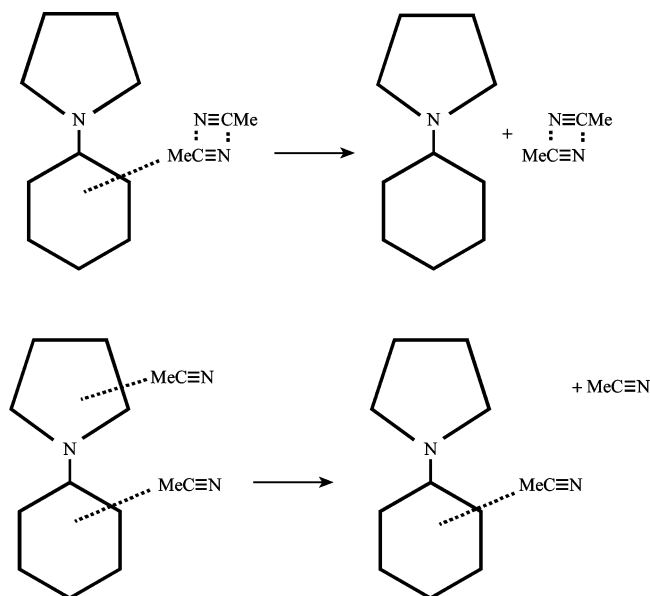


**Figure 10.** A schematic representation of two possible dissociation channels of isomeric  $PL_2$  clusters with the same stoichiometric composition but different geometry. Bottom: Single ligand dissociation,  $PL_2 \rightarrow PL + L$ . Top: Cluster ligand dissociation,  $(PL_2)^* \rightarrow P + L_2$ . The bond dissociation energies are similar in these two cases.

size of neutral clusters in the jet. Since no red-band emission is observed when the largest cluster ion observed contains less than four AN molecules, it is safe to conclude that clusters having up to three AN molecules are not transformed to the CT state upon light absorption.

**IV.e. The Role of Neutral PBN Dimers.** Dimers are easily formed in supersonic expansions. Their concentration can be controlled by varying the pressure of the monomer in the expanding gas mixture (in the present experiments, by adjusting the oven's temperature). When AN is added, a competition between dimer and heterocluster formation determines the relative concentration of the dimer, and of solvated dimers. Inspection of Figures 2 and 4 shows that the PBN dimer ion signal was below the noise level when the oven's temperature was set to 372 K, while at 399 K the dimer ion signal was clearly detected. It is very likely that the emission spectra of Figure 4 contain a contribution from solvated dimers, although the spectral bands centered at 460 nm are very similar to those of Figure 2 where

the dimers are absent. There appears to be a slight blue shift of the spectrum with the largest AN concentration.

## V. Comparison with Previous Work: The Absence of CT Emission from $PP(AN)_n$ Clusters

The conversion of the LE state to a CT one does not take place in the bare molecules. The potential surface of the reaction in solution is still under debate, and even the barrier for the process is not well established. In fact, it has been suggested that the process is entropy controlled in the case of DMABN.<sup>2,36,37</sup> In condensed phases the interaction between neighboring molecules is strongly affected by the cage effect; once formed, the CT state is likely to relax to the bottom of the potential well and can be observed by its characteristic emission. In clusters the dissociation option is much more important: the binding energy of the ligand to PBN or PP is only 2–5 kcal/mol, and dissociation can easily preclude the transition to the CT state. We interpret our results (the observation of CT emission for PBN/AN clusters and its absence in the case of PP/AN ones) as signifying that the binding of PBN to acetonitrile is stronger than that between two AN molecules, while in the case of PP the reverse is true. This may be attributed to the ordering of the dipole moments in the ground states of these molecules:  $\mu_{AN} \approx \mu_{PBN} > \mu_{PP}$ .<sup>38</sup> The polarizability of the phenyl derivatives is larger than that of AN, so that the van der Waals forces, dominated by dipole–dipole and induced dipole interactions are expected to be stronger for the PBN/AN pair than for the PP/AN one. Thus, when a PBN·(AN)<sub>n</sub> cluster is excited to higher vibrational levels of the LE state, it is more likely to cross to the CT state (while retaining the solvation layer) than to dissociate. In the case of a PP·(AN)<sub>n</sub> cluster, it will tend to eject one or more AN molecules rather than cross to the CT state. If  $P^{CT}$  molecules are directly excited, the Franck–Condon principle predicts vibrational excitation making probable the dissociation of the cluster. In the case of  $PP(AN)_n$  clusters, the rate of this process must be greater than  $k_{f,CT}$  (eq 4), while for PBN(AN)<sub>n</sub> clusters, it appears to be smaller.

In a more rigid environment, such as an argon matrix (with AN present), PP is found to exhibit dual fluorescence: a CT-type fluorescence band is clearly observed, separate from the LE band.<sup>19</sup> PBN under similar conditions exhibits a single, broad, emission band.<sup>39</sup> A tentative explanation is the following: the PP/AN pair is loosely bound in the argon matrix, but the pair cannot drift apart (cage effect). The CT state lies at a lower energy than in the gas phase, due to the polarizability of argon. Therefore, a smaller number of AN molecules is necessary than in the jet for the system to be transformed to the CT state. The very delicate energy balance involved is indicated by the sharp excitation energy dependence of the emission spectrum. In contrast with the solution spectra, direct excitation of the CT state appears to be possible in the red edge of the absorption spectrum.

The case of the PBN/AN system in a cryogenic solid is different. The binding of PBN to AN is much stronger, and the restriction on nuclear motion more severe. Therefore when the system crosses over to the CT state, relaxation to lower energy is restricted, and the CT emission is shifted to shorter wavelengths. A similar effect of the restricted relaxation in a solid matrix was discussed by Kasha et al.<sup>40</sup> Some support for this model is found by preliminary results in a xenon matrix: the emission band is observed to be shifted to longer wavelengths compared to the argon matrix. These results will be more extensively discussed in a forthcoming paper.<sup>39</sup>

The ion REMPI excitation spectra which we observed for PBN and PP AN clusters are similar to those published by

previous workers for DMABN clusters:<sup>14,15</sup> continuous and devoid of any vibrational structure. The most plausible explanation for these observations is the coexistence of many clusters in the jet, having different sizes and different shapes. They appear to emit similar spectra, and the decay times of their excited states are close enough to each other so that the overall decay is well fitted with a single exponential. More work is required to find out the actual structures of the clusters involved. Recent advances in quantum chemical calculations<sup>41,42</sup> appear to promise help in that regard.

## VI. Summary

The fluorescence of PBN clusters with acetonitrile (AN) was found to consist of two separate bands which by comparison with liquid solution are assigned to emission from LE and CT states. The CT emission is observed only for clusters containing more than a certain number of AN molecules. REMPI spectra run simultaneously with the fluorescence show that cluster ions of the type PBN·(AN)<sub>*n*</sub>, with *n* ≥ 4, are present when CT emission is observed, while when only smaller cluster ions are recorded, no CT emission is detected. It is not possible at this time to determine whether a neutral PBN·(AN)<sub>4</sub> cluster is large enough for CT formation to take place, as the cluster ions observed may be formed by dissociation of larger ones. Energy considerations indicate that 4 to 6 AN molecules are required for the CT emission to appear. CT-type emission was observed for these clusters when excited on the red edge of the absorption band; to our knowledge, no similar observation was reported to date on jet-cooled systems.

PP differs from PBN in that the electron acceptor is weaker, being a phenyl ring, rather than a cyanophenyl one. In liquid AN solution, PP is known to form a CT state. In the jet, no CT emission was observed even when the corresponding REMPI spectrum indicated the presence of large PP·(AN)<sub>*n*</sub> clusters. Probable reasons for the absence of CT emission in this case are (a) the facile dissociation of energized LE PP·(AN)<sub>*n*</sub> clusters, made possible by the weaker bonding of PP to AN compared to PBN, or (b) insufficient stabilization of the CT state in PP·(AN)<sub>*n*</sub> clusters.

**Acknowledgment.** We thank Drs. S. Zilberg, W. Fuss, and K. Zachariasse for many useful discussions and Mr. H. Baumgarten for his technical help. This research was supported by the Israel Science Foundation and by The Volkswagen-Stiftung (I/76 283). The Farkas Center for Light Induced Processes is supported by the Minerva Gesellschaft mbH.

## References and Notes

- (1) Lippert, E.; Lüder, W.; Boos, H. In *Advances in Molecular Spectroscopy*; Mangini, A., Ed.; Proceedings of the 4th International Meeting on Molecular Spectroscopy; Pergamon: Oxford, UK, 1962; p 443.
- (2) Grabowski, Z. R.; Rotkiewicz, K.; Rettig, W. *Chem. Rev.* **2003**, *103*, 3899.
- (3) Rotkiewicz, K.; Grellman, K. H.; Grabowski, Z. R. *Chem. Phys. Lett.* **1973**, *19*, 315. Grabowski, Z. R.; Rotkiewicz, K.; Siemiarz, A.; Cowley, D. J.; Baumann, W. *Nouv. J. Chim.* **1979**, *3*, 443.
- (4) Zachariasse, K. A.; Grobys, M.; von der Haar, Th.; Hebecker, A.; Il'chev, Yu. V.; Jiang, Y.-B.; Morawski, O.; Kühnle, W. *J. Photochem.*

- Photobiol. A: Chem.* **1996**, *102*, 59. Zachariasse, K. A.; Grobys, M.; von der Haar, Th.; Hebecker, A.; Il'chev, Yu. V.; Jiang, Y.-B.; Morawski, O.; Kühnle, W. *J. Photochem. Photobiol. A: Chem.* **1997**, *105*, 373.
- (5) Serrano-Andres, L.; Merchan, M.; Roos, B. O.; Lindh, R. *J. Am. Chem. Soc.* **1995**, *117*, 3189.
- (6) Parusel, A. B. *Phys. Chem. Chem. Phys.* **2000**, *2*, 5545.
- (7) Sudholt, W.; Staib, A.; Sobolewski, A.; Domcke, W. *Phys. Chem. Chem. Phys.* **2000**, *2*, 4341.
- (8) Zilberg, S.; Haas, Y. *J. Phys. Chem. A* **2002**, *104*, 1.
- (9) Polimeno, A.; Barbon, A.; Nordio, P. L.; Rettig, W. *J. Phys. Chem.* **1994**, *98*, 12158.
- (10) Fonseca, T.; Kim, H. J.; Hynes, J. T. *J. Mol. Liq.* **1994**, *60*, 161. Kim, H. J.; Hynes, J. T. *J. Photochem. Photobiol. A* **1997**, *105*, 337.
- (11) Proppe, B.; Merchan, M.; Serrano-Andres, L. *J. Phys. Chem. A* **2000**, *104*, 1608.
- (12) See for instance: *Chem. Rev.* **1994**, *94* (7), 1723–2160. *Chem. Rev.* **2000**, *100* (11), 3861–4264. Special issue on cluster physics and chemistry: *Chem. Phys.* **1998**, *239*, 1–620.
- (13) Howell, R.; Phillips, D.; Petek, H.; Yoshihara, K. *Chem. Phys.* **1994**, *188*, 303.
- (14) Krauss, O.; Lommatzsch, U.; Lahmann, C.; Brutchy, B.; Rettig, W.; Herbich, J. *Phys. Chem. Chem. Phys.* **2001**, *3*, 74.
- (15) Saigusa, H.; Iwase, E.; Nishimura, M. *J. Phys. Chem. A* **2003**, *107*, 3759, 4989.
- (16) Sarkar, A.; Chakravorti, S. *Chem. Phys. Lett.* **1995**, *235*, 195.
- (17) Cornelissen-Gude, C.; Rettig, W. *J. Phys. Chem. A* **1998**, *102*, 7754.
- (18) Yoshihara, T.; Galiewsky, V. A.; Druzhinin, S. I.; Saha, S.; Zachariasse, K. A. *Photochem. Photobiol. Sci.* **2003**, *2*, 342.
- (19) Schweke, D.; Haas, Y. *J. Phys. Chem. A* **2003**, *107*, 9554.
- (20) Wiley, W. C.; McLaren, I. H. *Rev. Sci. Instrum.* **1955**, *26*, 1150.
- (21) Rettig, W.; Marschner, F. *New Chem. J.* **1990**, *14*, 819.
- (22) Kandler, S.; Haas, Y. *J. Phys. Chem. A* **1997**, *101*, 2578. Kandler, S.; Haas, Y. *Chem. Phys. Lett.* **1995**, *236*, 324.
- (23) Due to the small size of the aperture in front of the Daly detector, small and large masses cannot be simultaneously monitored. The mass spectra shown in Figure 2 were obtained by recording at various deflector voltages and summing over all spectra obtained.
- (24) Belau, L.; Haas, Y.; Rettig, W. *Chem. Phys. Lett.* **2002**, *364*, 157.
- (25) Klotz, C. E. *J. Chem. Phys.* **1985**, *83*, 5854.
- (26) Neusser, H. J.; Krause, H. *Chem. Rev.* **1994**, *94*, 1829.
- (27) Ohashi, K.; Nakane, Y.; Inokuchi, Y.; Nakai, Y.; Nishi, N. *Chem. Phys.* **1998**, *239*, 429.
- (28) Braun, J.; Neusser, H. J.; Hobza, P. *J. Phys. Chem. A* **2003**, *107*, 3918.
- (29) Haas, Y.; Kandler, S. *Isr. J. Chem.* **1997**, *37*, 427.
- (30) Shang, Q.; Bernstein, E. R. *J. Chem. Phys.* **1992**, *97*, 80.
- (31) Wickelder, C.; Droz, T.; Bürgi, T.; Leutwyler, S. *Chem. Phys. Lett.* **1997**, *264*, 257.
- (32) Brutschy, B. *Chem. Rev.* **2000**, *100*, 3891.
- (33) Liptay, W. *Z. Naturforsch.* **1965**, *20a*, 1441.
- (34) Boettcher, C. J. F. *Theory of Electric Polarization*; Elsevier: Amsterdam, The Netherlands, 1973; Chapter 4.
- (35) Rettig, W.; Marschner, F. *Nouv. J. Chim.* **1983**, *7*, 425.
- (36) Rettig, W. *Ber. Bunsen-Ges. Phys. Chem.* **1991**, *95*, 259.
- (37) Rettig, W.; Fritz, R.; Braun, D. *J. Phys. Chem. A* **1997**, *101*, 6830.
- (38) The dipole moment of AN is 3.92 D (*Handbook of Chemistry and Physics*, 60th ed.; CRC Press: Boca Raton, FL, 1980; p E-64). The calculated dipole moments with use of DFT (B3LYP/cc-pVDZ) are 3.72, 3.67, and -1.50 D for AN, PBN, and PP, respectively.
- (39) Schweke, D.; Baumgarten, H.; Haas, Y.; Rettig, W. Unpublished results. The emission spectrum of PBN in an argon matrix shows a broad band peaking around 300 nm, extending to about 500 nm with a little vibronic structure on the blue side. Addition of AN to the matrix leads to a very similar spectrum, devoid of vibronic structure, and a somewhat increased intensity in the red edge. In contrast with similarly prepared PP matrices, two separate bands are not observed.
- (40) Kasha, M.; Sytnik, A.; Dellinger, B. *Pure Appl. Chem.* **1993**, *65*, 1641.
- (41) Kim, K. S.; Tarakeshwan, P.; Lee, J. T. *Chem. Rev.* **2000**, *100*, 4145.
- (42) Sinnokroft, M. O.; Valeev, E. F.; Sherrill, C. D. *J. Am. Chem. Soc.* **2002**, *124*, 10887.